SIMULATION OF LASER MELTING AND EVAPORATION OF SUPERCONDUCTING CERAMICS

V. Mazhukin
Institute of Mathematical Modeling, Russian Academy of Sciences, Miusskaya Square, 4, 125047 Moscow, Russia

I. Smurov
Ecole Nationale d'Ingénieurs de Saint-Etienne, 58, rue Jean Parot, 42023 Saint-Etienne Cedex 2, France

C. Dupuy
Institut de Science et de Génie des Matériaux et Procédés, Centre National de la Recherche Scientifique, B.P.5 Odeillo, 66125 Font-Romeu, France

D. Jeandel
Laboratoire de Mécanique des Fluides et d'Acoustique, Centre National de la Recherche Scientifique, Ecole Centrale de Lyon, B.P. 163, 69131 Ecully, France

The peculiarities of pulsed laser melting and evaporation of the superconducting ceramics are analyzed by means of numerical simulation. The appearance of the overheated metastable states in solid and liquid phases is shown as a result of the phase front dynamics and volume nature of laser energy release. A method of dynamic adaptation for the multifront Stefan problem is proposed.

INTRODUCTION

Pulsed laser deposition (PLD) of thin superconducting films for electronic device applications (e.g., compact high-quality factor filters, delay lines, and Josephson elements for high-speed, low-power switching) is a modern and successfully developing technology [1–3]. In the typical experiments, the 20- to 30-ns-wide laser pulse is focused to an energy density (usually in the range 1–10 J/cm^2) to vaporize a few hundred Angstroms of surface material, which then is deposited onto the substrate. By generating high peak powers, congruent evaporation, which is the most important virtue of PLD, was observed in many systems from simple

Received 2 December 1992; accepted 29 December 1993.
Address correspondence to I. Smurov, Ecole Nationale d'Ingénieurs de Saint-Etienne, 58, rue Jean Parot, 42023 Saint-Etienne Cedex 2, France.

Numerical Heat Transfer, Part A, 26:587–600, 1994

1040–7782/94 $10.00 + .00

NOMENCLATURE

a	thermal diffusivity	v_{lv}	velocity of liquid-vapor interface
$A(T_s)$	surface absorptivity	x	spatial coordinate
C_p	heat capacity	x_0, x_L	limits of coordinate variation
G	energy density flux	γ	ratio of heat capacities
G_s	absorbed energy density flux	Γ_{sl}	solid-liquid interface
G_0	maximum value of incident energy density flux	Γ_{lv}	liquid-vapor interface
		κ	coefficient of volumetric absorption of laser radiation
L_m	latent heat of melting		
L_v	latent heat of evaporation		
M	Mach number	λ	coefficient of heat conductivity
P	pressure	ρ	density
R	universal gas constant		
t	time	**Subscripts**	
$-t_0, t^J$	the limits of time variation		
$T(x,t)$	temperature	b	boiling point
T_m	melting point	H	saturated vapor
T_0	initial temperature	l	liquid phase
u	vapor velocity	s	condensed phase
v_{sl}	velocity of solid-liquid interface	v	gas phase

ternary compounds to low-temperature superconductors with quite complex stoichiometry.

The related physical phenomena include volume absorption of laser radiation, heating, melting, and evaporation of the target's material, plasma formation, and finally, the deposition of thin films on a substrate in a vacuum chamber (100–300 mtorr of oxygen). The micron-sized particles generated by splashing are a major detriment to film quality.

The application of such treatment operations as laser surface remelting and annealing of ceramics is also widely used to obtain the required properties of surface layers (for example, Ref. [4]). The main problem in these operations is inaccurate prediction of results due to incompletely known physics of the processes. The formation of gas bubbles, volume type of evaporation, etc., make the process of laser treatment rather complicated.

On the other hand, ceramics are materials with complex chemical composition whose optical and thermophysical characteristics have not been fully studied, making it difficult to determine the optimum modes of influence. The role of mathematical modeling in such situations is considerably increased.

In the present article a possible reason for micron-sized particle generation by splashing in PLD is proposed and analyzed by means of numerical experiments.

FORMULATION OF THE PROBLEM

Laser radiation is spread along the x axis from right to left (Figure 1). Solid-liquid and liquid-vapor interfaces are located at points $x = \Gamma_{sl}$ and $x = \Gamma_{lv}$. Upon reaching the material surface, the laser flux is partially absorbed, and the

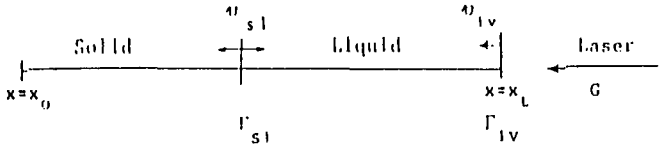

Figure 1. Scheme of the physical model.

result is heating, melting, or evaporation, depending on the intensity and pulse duration.

Surface and Volume Energy Absorption

The volume and surface energy absorption of electromagnetic radiation can be distinguished with respect to correlations between absorption coefficient κ and thermal influence length $l_T \sim (at)^{1/2}$. If the thermal influence length is much more than the quantum run length in the medium $l_p \sim \kappa^{-1}$ ($l_T \gg l_p$), the mechanism for radiation transformation into thermal energy has a surface nature. On the contrary, if $l_T \leq l_p$, energy absorption occurs volumetrically. The volumetric nature of heating could also take place with phase transformation if $\kappa a/v_{sl} \leq 1$, i.e., if the energy absorption length is not small in comparison with the thermal influence length for a moving phase boundary.

The volume absorption of laser radiation is described by the system containing an energy equation and an equation for radiation transfer:

$$C_p(T)\rho(T)\frac{\partial T}{\partial t} = \frac{\partial}{\partial x}\lambda(T)\frac{\partial T}{\partial x} - \frac{\partial G}{\partial x} \tag{1}$$

$$\frac{\partial G}{\partial x} + \kappa G = 0 \tag{2}$$

On the irradiated surface $x = x_L$, the following boundary conditions are written:

$$x = x_L: \quad \lambda\frac{\partial T}{\partial x} = 0 \qquad G_s = A(T_s)G_0 \tag{3}$$

With the occurrence of surface energy absorption the heat transfer equation, Eq. (1), does not contain the term $\partial G/\partial x$, i.e., the equation for radiation transfer is not required. In this case, laser action is taken into account in the boundary condition (Eq. (3)) presented as the law of energy conservation.

Mathematical Model

Taking into consideration the above statements, the mathematical model describing the behavior of solid (s) and liquid (l) phases accounting for phase

transformations can be written as follows [5]:

$$\left[C_p(T)\rho(T)\frac{\partial T}{\partial t}\right]_k = \left[\frac{\partial}{\partial x}\lambda(T)\frac{\partial T}{\partial x} - \frac{\partial G}{\partial x}\right]_k \qquad k = \mathrm{s}, \mathrm{l}$$

$$\left[\frac{\partial G}{\partial x} + \kappa G\right]_k = 0 \qquad -t_0 < t < t^J \qquad x_0 < x < x_{\mathrm{L}} \tag{4}$$

with boundary conditions

$$t = 0: \qquad T(x,0) = T_0$$

$$x = x_0: \qquad \lambda\frac{\partial T}{\partial x} = 0$$

$$x = \Gamma_{\mathrm{sl}}: \qquad \lambda_{\mathrm{s}}\frac{\partial T_{\mathrm{s}}}{\partial x} - \lambda_{\mathrm{l}}\frac{\partial T_{\mathrm{l}}}{\partial x} = \rho_{\mathrm{l}} L_{\mathrm{m}} v_{\mathrm{sl}} \qquad T_{\mathrm{s}} = T_{\mathrm{l}} = T_{\mathrm{m}} \tag{5}$$

$$x = \Gamma_{\mathrm{lv}}: \; -\lambda_{\mathrm{l}}\frac{\partial T_{\mathrm{l}}}{\partial x} = \rho_{\mathrm{l}} L_{\mathrm{v}} v_{\mathrm{lv}} \qquad G_{\mathrm{s}} = A(T_{\mathrm{s}})G_0 \exp\left[-\left(\frac{t}{\tau}\right)^2\right]$$

$$\rho_{\mathrm{l}} v_{\mathrm{lv}} = \rho_{\mathrm{v}}(v_{\mathrm{lv}} - u)$$

$$P_{\mathrm{l}} + \rho_{\mathrm{l}} v_{\mathrm{v}}^2 = P_{\mathrm{v}} + \rho_{\mathrm{v}}(v_{\mathrm{lv}} - u)^2$$

$$T_{\mathrm{v}} = T_{\mathrm{l}}\left\{\left[1 + \pi\left(\frac{\gamma-1}{\gamma+1}\frac{m}{2}\right)^2\right]^{1/2} - \pi^{1/2}\frac{\gamma-1}{\gamma+1}\frac{m}{2}\right\}^2$$

$$\rho_{\mathrm{v}} = \rho_{\mathrm{H}}\left\{\left(\frac{T_{\mathrm{l}}}{T_{\mathrm{v}}}\right)^{1/2}\left[\left(m^2 + \frac{1}{2}\right)\exp(m^2)\,\mathrm{erfc}(m) - \frac{m}{\pi^{1/2}}\right] + \frac{1}{2}\frac{T_{\mathrm{l}}}{T_{\mathrm{v}}}\left[1 - \pi^{1/2} m \exp(m^2)\,\mathrm{erfc}(m)\right]\right\} \tag{6}$$

$$m = \frac{u}{(2RT_{\mathrm{v}})^{1/2}} \qquad M = m\left[\frac{2}{\gamma}\right]^{1/2}$$

$$P_{\mathrm{H}} = R\rho_{\mathrm{H}}T_{\mathrm{l}} \qquad P_{\mathrm{H}} = P_{\mathrm{b}}\exp\left[\frac{L_{\mathrm{v}}}{RT_{\mathrm{l}}}\left(1 - \frac{T_{\mathrm{b}}}{T_{\mathrm{l}}}\right)\right]$$

The evaporation process is described within the approximation of the Knudsen layer, presented as the gas-dynamic discontinuity on the phase boundary at $x = \Gamma_{\mathrm{lv}}$, where three conservation laws (energy, mass, and momentum, respectively) and two additional relations (characterized by the nonequilibrium degree of the

phase boundary) are used [6]. In the present work, evaporation into a vacuum is considered; as a result, $M = 1$.

METHOD OF NUMERICAL SOLUTION

The numerical algorithm is based on the method of dynamic adaptation of computational grids for the solution to be determined (especially developed for Stefan problems [7, 8]). This method is used for the solution of the problem Eqs. (4)–(6) and allows us to analyze both one-dimensional and multidimensional tasks [9]. In the dynamic adaptation methods the problem for computational grid construction is formulated at a differential level. In the differential problem, one part of the equations describes physical processes, and the other part describes the behavior of the grid points.

General Introduction

The main difficulty in the solution of Stefan problems is connected with the presence of moving boundaries, the position of which is determined during the solution. The dynamic adaptation method is based on the procedure of transition to an arbitrary transient coordinate system by means of its automatic transformation with the help of the solution to be determined. The transition to a transient coordinate system allows us to eliminate the problems related to moving boundaries. In this case it is necessary to determine not only the grid functions but also the coordinates of the grid points. The grid point behavior is determined by the partial differential equations (their amount is defined by the number of independent variables), which are added to the initial mathematical model. In the proposed method the adaptation mechanism of computational grids is introduced at the differential level and does not depend on the method for numerical realization of mathematical models (finite differences or finite elements). The behavior of the additional equations depends on the dynamics of the physical process. The transformation of coordinates by means of the solution to be determined, allows us to dislocate grid points depending on the solution peculiarities. Such peculiarities can be as follows: spreading of large gradients, shock waves, contact and phase boundaries. Thickening of points in the regions of strong variation of the solution is done by a transformation function Q, which in a general case could be a combination of the numerical solution and its derivatives [10, 11].

The problems connected with moving boundaries are eliminated by the transition to an arbitrary transient system of coordinates in which grid points and boundaries appear to be unmovable. In this respect, the method is similar to Lagrangian methods. However, there is a principal difference. In Lagrangian methods, hydrodynamic velocity is speeded up for the transient system of coordinates. This is not always convenient and considerably narrows the class of problems to be solved. In the dynamic adaptation methods, the velocity of the coordinate system (and grid point distribution) is not indicated beforehand. It is defined during the problem solution and depends on the peculiarities of the solution to be determined. It principally allows us to obtain any desired point distribution, and the application of the method is not limited by the problems of phase front

dynamics, hydrodynamics, or gas dynamics. A more complete discussion of the principles for constructing dynamically adapting algorithms for transient boundary value problems is given in Ref. [12].

It is necessary to emphasize that different methods of construction of computational grids are developed on the basis of various adaptation mechanisms (for example, Refs. [13–16]). Also notice should be taken of the fact that the simulation of the Stefan type problems with the volume energy release should be done by the explicit tracking of phase front positions.

Dynamic Adaptation Method

Let us formulate the method for numerical solution with dynamic adaptation for the system Eqs. (4)–(6). Transition to an arbitrary system of coordinates is done by substitution of variables of the general type:

$$x = f(q, \tau) \qquad t = \tau$$

having the reverse transformation

$$q = \Phi(x, t) \qquad \tau = t$$

Partial derivatives of dependent variables are expressed conventionally:

$$\frac{\partial}{\partial t} = \frac{\partial}{\partial \tau} + \frac{\partial q}{\partial \tau}\frac{\partial}{\partial q} = \frac{\partial}{\partial \tau} - \frac{\partial x}{\partial \tau}\frac{\rho}{\Psi}\frac{\partial}{\partial q} = \frac{\partial}{\partial \tau} + \frac{Q}{\Psi}\frac{\partial}{\partial q}$$

$$\frac{\partial}{\partial x} = \frac{\partial q}{\partial x}\frac{\partial}{\partial q} = \frac{\rho}{\Psi}\frac{\partial}{\partial q} \qquad \Psi = \frac{\partial x}{\partial q}\rho$$

where $\partial x/\partial \tau = -Q/\rho$ is the velocity of the coordinate system, Q is an arbitrary function depending on the solution to be determined, and Ψ is the metric coefficient (or transformation coefficient) indicating how many times the initial area is changed.

Using substitution of variables, the mathematical model Eqs. (4)–(6) can be written in variables q, τ, representing differential equations in divergent form:

$$\left(\frac{\partial(H\Psi)}{\partial \tau}\right)_k = -\left(\frac{\partial W}{\partial q} + \frac{\partial(QH)}{\partial q} + \frac{\partial G}{\partial q}\right)_k \qquad H = C_p T \tag{7}$$

$$\left(\frac{\partial G}{\partial q} + \lambda^{-1}\rho\Psi G = 0\right)_k \qquad W = -\frac{\rho\lambda}{\Psi}\frac{\partial T}{\partial q} \tag{8}$$

$$\left(\frac{\partial \Psi}{\partial \tau} = -\frac{\partial Q}{\partial q}\right)_k \frac{\Psi}{\rho} = \frac{\partial x}{\partial q} \qquad k = \mathrm{s}, \mathrm{l} \qquad q_0 < q < q_L \tag{9}$$

The boundary conditions are

$$t = 0: \qquad T(q,0) = T_0$$

$$q = q_0: \qquad \frac{\lambda\rho}{\Psi}\frac{\partial T}{\partial q} = 0 \qquad Q = 0$$

$$q = \Gamma_{sl}: \qquad T_s = T_l = T_m \qquad Q_{sl} = -\rho_s v_{sl} \qquad Q_{sl} = +\frac{W_s - W_l}{L_m} \tag{10}$$

$$q = \Gamma_{lv}: \qquad \frac{\lambda_l \rho_l}{\Psi_l}\frac{\partial T_l}{\partial q} = -L_v Q_{lv}$$

$$G_s = A(T_s)G_0 \exp\left[-\left(\frac{t}{\tau}\right)^2\right]$$

$$\rho_l v_{lv} = \rho_v(v_{lv} - u) \qquad Q_{lv} = -\rho_l v_{lv}$$

$$P_l + \rho_l v_{lv}^2 = P_v + \rho_v(v_{lv} - u)^2$$

$$T_v = T_l\left\{\left[1 + \pi\left(\frac{\gamma-1}{\gamma+1}\frac{m}{2}\right)^2\right]^{1/2} - \pi^{1/2}\frac{\gamma-1}{\gamma+1}\frac{m}{2}\right\}^2$$

$$\rho_v = \rho_H\left\{\left(\frac{T_l}{T_v}\right)^{1/2}\left[\left(m^2 + \frac{1}{2}\right)\exp(m^2)\,\mathrm{erfc}(m) - \frac{m}{\pi^{1/2}}\right]\right.$$

$$\left. + \frac{1}{2}\frac{T_l}{T_v}\left[1 - \pi^{1/2} m \exp(m^2)\,\mathrm{erfc}(m)\right]\right\} \tag{11}$$

Equation (9) is the equation of reverse transformation. Function Q in this equation, as already noted, depends on pecularities of the solution to be determined. Q thus permits a grcat freedom of choice to the user. Briefly, in terms of the choice of Q (special analysis is done in Ref. [12]), it should be noted that some typical forms of Q functions will lead to different typical transformations. For example, choosing Q based on the velocity of the solution variation makes it possible to obtain the thickening of grid points in the region of large gradients [10–12]. As shown in practice, for the problem with moving boundaries the most convenient form is $Q = -D(\partial\psi/\partial q)$. This provides a quasi-uniform grid with fixed number of points at each time step, if the value of coefficient D is optimum. Thus, the problem for moving interface boundaries in computational space leads to the determination of Q_{sl}, Q_{lv} values.

Computational Grid

To construct discrete models that approximate differential statements of the problem Eqs. (7)–(11), computational grids W_i^j are introduced in each phase subregion. Computational grids with nonuniform step h_i along spatially variable q and step $\Delta\tau^j$ along variable τ are used in the solid phase:

$$\omega = \Big\{(q_i, \Delta\tau^j), \big(q_{i+1/2}, \Delta\tau^j\big), q_{i+1} = q_i + h_i,$$

$$q_{i+1/2} = q_i + 0.5h_i; \tau^{j+1} = \tau^j + \Delta\tau^j,$$

$$i = 0, 1, \ldots, N, \quad j = 0, 1, \ldots, J\Big\}$$

In the region of the liquid phase, a uniform-space grid is used.

Construction of discrete models in each subregion was done by implicit conservative difference schemes:

$$\left[\frac{(\Psi H)_{i+1/2}^{j+1} - (\Psi H)_{i+1/2}^{j}}{\Delta\tau^{j+1}} = -\frac{W_{i+1}^{j+1} - W_i^{j+1}}{h_i}\right.$$

$$\left. - \frac{(QH)_{i+1}^{j+1} - (QH)_i^{j+1}}{h_i} - \frac{G_{i+1}^{j+1} - G_i^{j+1}}{h_i}\right]_k$$

$$\left[\frac{\Psi_{i+1/2}^{j+1} - \Psi_{i+1/2}^{j}}{\Delta\tau^{j+1}} = -\frac{Q_{i+1}^{j+1} - Q_i^{j+1}}{h_i}\right]_k$$

$$\left(\frac{G_{i+1} - G_i}{h_i} + \kappa(\Psi\tilde{\rho}^{-1}\tilde{G})_{i+1} = 0\right)_k^{j+1} \qquad k = \mathrm{s}, \mathrm{l} \tag{12}$$

$$\frac{x_{i+1}^{j+1} - x_i^{j+1}}{h_i} = \frac{\Psi_{i+1/2}^{j+1}}{\rho_{i+1/2}^{j+1}} \qquad Q_i^j = -D\frac{\Psi_{i+1/2}^{j} - \Psi_{i-1/2}^{j}}{h_i h_{i-1}}$$

$$W_i^j = -\left[\frac{\lambda_i^j \rho_i^j}{\Psi_i^j}\left(\frac{T_{i+1/2}^j - T_{i-1/2}^j}{h_i h_{i-1}}\right)\right] \qquad i = 0, 1, 2, \ldots, N-1$$

Functions $W_i^j, Q_i^j, x_i^j, \lambda_i^j, C_{pi}^j$ are related to nodes, and $T_{i+1/2}^j, \Psi_{i+1/2}^j$ to points between nodes.

Values T_i^j, Ψ_i^j in nodes were determined through the values of these functions in points between nodes by the interpolation formula

$$y_i^j = \frac{\rho_{i+1/2}^j \Psi_{i-1/2}^j h_{i-1/2} y_{i+1/2}^j + h_{i+1/2} y_{i-1/2}^j \Psi_{i+1/2}^j \rho_{i-1/2}^j}{\rho_{i+1/2}^j \Psi_{i-1/2}^j h_{i-1/2} + h_{i+1/2} \Psi_{i+1/2}^j \rho_{i-1/2}^j}$$

SOLUTION ALGORITHM

The application of dynamic adaptation allowed us to develop a numerical algorithm of which the main idea is to make calculations according to a shock-fitting scheme with simultaneous front tracking [17]. For this purpose the solution of the difference scheme Eq. (12) at one time step τ^j is done by means of two enclosed iteration cycles. In the first, boundary condition values Q_{sl} and Q_{lv} are determined by iteration procedures. This is equivalent to the determination of phase front velocities v_{sl}, v_{lv}. In the second cycle, for both regions the values for temperature T_i^j and function Ψ_i^j are determined by the widely used Gaussian method for three diagonal matrices combined with the Newton-Raphson method. Iterations were executed to fulfill the conditions

$$|\delta\Psi_i^s| = |\Psi_i^{s+1} - \Psi_i^s| < \varepsilon_1\Psi_i^s + \varepsilon_2$$
$$|\delta T_i^s| = |T_i^{s+1} - T_i^s| < \varepsilon_3 T_i^s + \varepsilon_4 \qquad \varepsilon_1 - \varepsilon_4 \leq 10^{-3} - 10^{-5}$$

Certain difficulties can arise in the case of a new phase formation. In the present method, a new region was introduced by the following procedure. During heating, the solid phase surface was allowed to overheat (above the melting point) not more than 0.2 K. It is assumed that energy consumed for overheating is necessary to form the liquid phase. The initial liquid thickness and initial velocity approximation, v_{sl}, are determined by comparing the overheating energy with the phase transformation energy. The value of overheating (0.2 K) is chosen in such a way that the conserved energy is enough for melting several atomic layers. Usually, the new phase thickness is in the range 10–100 Å.

ANALYSIS OF THE SIMULATION RESULTS

Consider the typical conditions of pulsed laser evaporation of ceramics, series $YBa_2Cu_3O_{7-x}$. From experience, it is known that corresponding optical and thermophysical properties depend weakly on temperature and their values are within the range $\kappa = 10^6$–10^7 m^{-1}, $C_p = (3\text{–}8) \times 10^2$ J/(kg K), $\lambda = 1$–5 W/(m K). Thus, ceramics materials, in comparison with metals, have low thermal diffusivity a and a relatively high absorption coefficient κ, as compared with dielectrics. The experiments show that ceramics, series $YBa_2Cu_3O_{7-x}$, evaporate through the melting state, i.e., similar to most metals. However, due to other relations between parameters a and κ, laser energy absorption in ceramics will be substantially of the volumetric type.

Because of the absence of reliable data on optical and thermophysical characteristics and parameters, in the calculations all the values are assumed to be constant and are the same for both phases:

$$T_m = 1300 \text{ K} \quad T_v = 2000 \text{ K} \quad L_m = 2.5 \times 10^5 \text{ J/kg} \quad L_v = 6 \times 10^6 \text{ J/kg}$$

$$\rho_s = \rho_l = 6.43 \times 10^3 \text{ kg/m}^3 \quad \lambda_s = \lambda_l = 3 \text{ W/(m K)} \quad A_s = A_l = 0.8$$

$$C_{p_s} = C_{p_l} = 5 \times 10^2 \text{ J/(kg K)} \quad \kappa = 5 \times 10^6 \text{ m}^{-1}$$

Note that the problem of examination of ceramics properties requires special consideration, which is not available in the present paper.

Consider some general regularities of ceramics (thickness 5 μm) melting and evaporation by laser pulse with the following parameters: $\tau = 50$ ns and $G_0 = 10^7$ W/cm^2. Note that the real time shape of a laser pulse is approximated by Gaussian law. This is why it is convenient to measure the time relative to the middle of the pulse. In this case the time before the middle of the pulse will be negative and after, positive. Because of the low conductivity (and short pulse duration) of ceramics, its initial thickness is large enough to neglect the boundary condition on the back side. Therefore, the heat processes considered correspond practically to the semi-infinite body.

The temperature profile $T(x)$ and distribution of the volumetric heat source $G(x)$ are shown in Figure 2. They are fixed just before the start of melting. The given profile $T(x)$ differs from the analogous one, to be obtained by surface source heating, in the smoother distributions in space and lower spatial gradients, resulting in slower increase of melting velocity V_{sl}. The melting process starts from the irradiated surface and rapidly leads to maximum temperature formation in the depth of the solid phase by the volumetric heat source (Figures 3 and 4). Its temperature is 50° over the melting point T_m. As a result, the region in the solid phase (about 0.5 μm) is formed where the substance is in an overheated metastable state. Sizes of the overheated region and the degree of overheating generally depend on thermal diffusivity, absorptivity, and heat source intensity. It is necessary to emphasize that the detection of the above-mentioned effect is not possible without explicit tracking of the melt front position. Overheating of the solid state in the case of laser action on metallic materials (with explicit tracking of the phase front positions) was not observed because of the surface energy absorption [18–20].

During heating, the thickness of the liquid phase increases rapidly, reaching 0.1 μm at the middle of the pulse (Figure 5). The increase of liquid phase thickness

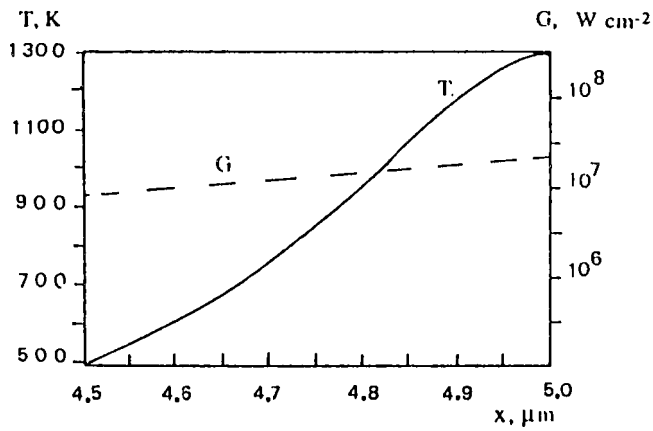

Figure 2. Spatial temperature distribution (T) before the beginning of melting, $t = -3.51 \times 10^{-8}$ s (approximately the middle of the pulse). Dashed curve shows the spatial distribution of the absorbed energy density flux G. Right boundary corresponds to the position of the irradiated surface.

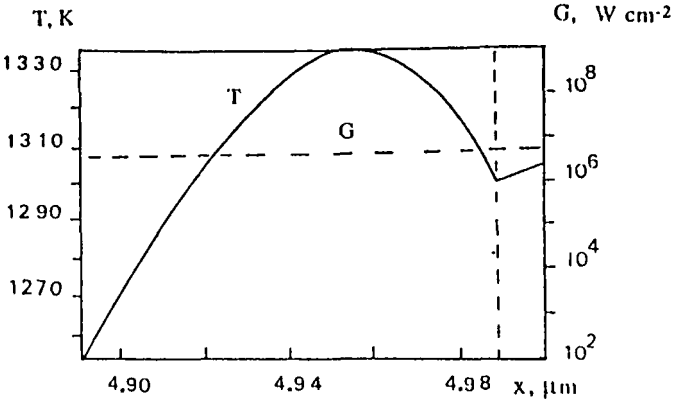

Figure 3. Same as Figure 2 but for the spatial temperature distribution (T) at $t = -3.24 \times 10^{-8}$ s. Vertical dashed line shows the position of the melting front.

leads to the fact that a great part of the radiation is absorbed in the melt, resulting in further heating, up to temperatures comparable to the boiling point. At the same time, a relatively small portion of radiation reaches the solid phase, and the degree of overheating (because of the heat transfer) is decreased until it completely disappears. In the liquid phase, surface evaporation on one hand and volume energy absorption on the other hand lead to the formation of a new metastable (relative to the pressure of its saturated vapor) region with maximum temperature at a certain distance from the surface (Figure 5). As distinct from solid phase overheating, the metastable state in liquid is maintained until the pulse ends. In the case of laser action on metallic materials, the subsurface maximum of temperature is absent (even when intensive evaporation takes place) because of surface energy absorption [18–20].

It is necessary to note that in the present heat model, Eqs. (4)–(6), the processes of volumetric liquid phase nucleation and volumetric vapor formation are not considered. Therefore, a detailed study of the kinetics of these phenomena is not possible. Moreover, it is supposed in the heat model that the metastable

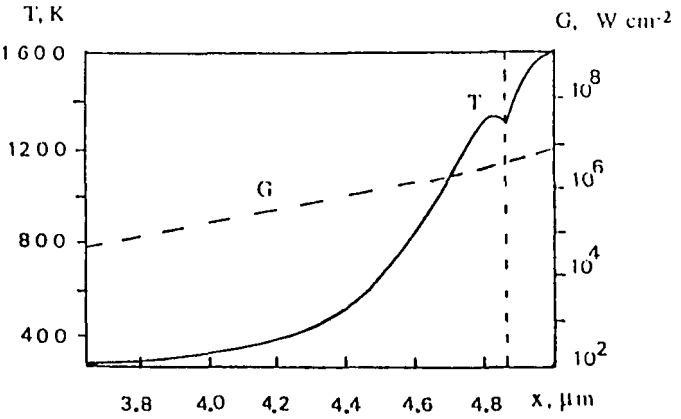

Figure 4. Same as Figure 3 but for the spatial temperature distribution (T) at $t = -2.19 \times 10^{-8}$ s.

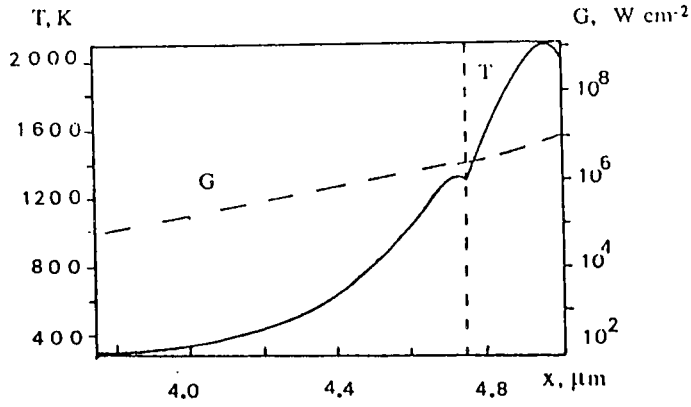

Figure 5. Same as Figure 3 but for the spatial temperature distribution (T) at $t = -9.17 \times 10^{-9}$ s. Intensive surface evaporation has induced the appearance of a subsurface temperature maximum.

phase is stable enough and does not decay during pulse action. Therefore, the given calculations are mainly to point out the possibility of the appearance of metastable regions during laser treatment. More attentive study of such phenomena requires additional experimental research and development of new mathematical models. At present, the practical importance is mainly that numerical simulation predicts the conditions for the appearance of metastable states. Though their lifetime is unknown, it is always finite. Therefore, explosive decay of the metastable phase due to volumetric vapor formation is actually possible; as a result, the liquid droplets can break down the deposition process based on laser evaporation. It is necessary to keep this process in mind for the development and application of laser technologies because an explosive decay of metastable states can not only accelerate the process of material elimination but can also create a serious problem during thin film deposition and obtainment of the submicron-sized elements.

CONCLUSION

1. The mathematical model takes into account the dynamics of phase fronts of melting (solidification) and evaporation under laser irradiation, which is absorbed volumetrically. The evaporation process is described within the approximation of the Knudsen layer, melting, on the basis of a Stefan-type boundary condition.
2. The numerical algorithm is based on the method of dynamic adaptation of computational grids for the solution to be determined (especially developed for Stefan problems). The velocity of the coordinate system (and grid point distribution) is not indicated beforehand but is defined during the problem solution and depends on the pecularities of the solution to be determined.
3. The appearance of the region in the solid phase whose temperature is higher than the melting point is shown. This is a consequence of the

volumetric nature of energy release on one hand and the melting phenomenon on the other hand, when the interface temperature is fixed. The lifetime, the sizes of the metastable region, and the degree of overheating generally depend on the phase front dynamics and nucleation processes.

4. The existence of a subsurface temperature maximum in the liquid phase is shown. This is the result of the volumetric nature of energy release, on one hand and the evaporation phenomenon on the other hand, when surface heat losses are essential.
5. The appearance of the overheated metastable states (in the range of parameters typical for PLD of superconducting films) can cause splashing and subsequent generation of micron-sized particles.
6. The present mathematical model may be used for heat phenomena simulation in pulsed and continuous laser action on a wide class of ceramic materials. The results obtained (such as solid phase overheating and subsurface temperature maximum in the liquid phase) may be generalized to other cases of laser radiation interaction with materials having a volume type of energy absorption.

REFERENCES

1. D. B. Chrisey and A. Inam, Pulsed Laser Deposition of High T_c Superconducting Thin Films for Electronic Device Applications, *MRS Bull.*, vol. 17, no. 2, pp. 37–43, 1992.
2. D. C. Paine and J. C. Bravman (eds.), Laser Ablation for Material Synthesis, *Mater. Res. Symp. Proc.*, vol. 191, 1990.
3. E. Fogarassy, C. Fuchs, and S. de Unamuno, High T_c Superconducting Thin Film Deposition by Laser Induced Forward Transfer, *Mater. Mfg. Processes*, vol. 7, no. 1, pp. 31–51, 1992.
4. I. Smurov, A. Uglov, Yu. Krivonogov, S. Sturlese, and C. Bartuli, Pulsed Laser Treatment of Plasma-Sprayed Thermal Barrier Coatings: Effect of Pulse Duration and Energy Input, *J. Mater. Sci.*, vol. 27, no. 16, pp. 4523–4530, 1992.
5. G. Carslaw and D. Jaeger, *Conduction of Heat in Solids*, 2nd ed., Oxford University Press, Oxford, 1959.
6. C. J. Knith, Theoretical Modeling of Rapid Surface Vaporization with Back Pressure, *AIAA J.*, vol. 17, no. 5, pp. 519–523, 1979.
7. N. A. Dar'in and V. I. Mazhukin, Mathematical Modeling of Stefan Problem Using Adaptive Grids, *Differenzialnue Uravnenija*, vol. 23, no. 7, pp. 1154–1160, 1987.
8. P. V. Breslavskij and V. I. Mazhukin, Mathematical Modeling of Pulse Melting and Evaporation of Metals with the Explicit Tracking of Phase Fronts, *Inzh. Fiz. Zh.*, vol. 57, no. 1, pp. 107–114, 1989.
9. V. I. Mazhukin, Mathematical Modeling of Stefan Problems by Means of Adaptive Grids, Proceedings of Int. Conf. MMF/HEAT/MASS TRANSFER-MIF/, Minsk, pp. 125–139, 1988.
10. N. A. Dar'in and V. I. Mazhukin, About One Approach to Construct the Adaptive Difference Grids, *DAN SSSR*, vol. 298, no. 1, pp. 64–68, 1988.
11. V. F. Vasilevskij and V. I. Mazhukin, Numerical Calculation of Temperature Waves with Weak Break by Dynamic Adaptive Grids, *Differenzialnue Uravnenija*, vol. 25, no. 7, pp. 1188–1193, 1989.
12. V. I. Mazhukin and L. Ju. Takojeva, The Construction Principles of the Grids Dynamically Adapted to the Solution, *Math. Modelirovanie*, vol. 2, no. 3, pp. 101–118, 1990.

13. J. F. Thompson, Grid Generation Technique in Computation Fluid Dynamics, *AIAA J.*, vol. 22, no. 11, pp. 1505–1523, 1984.
14. J. G. Verner, J. G. Blom, and J. M. Sanz-Serna, An Adaptive Moving Method for One-Dimensional Systems of Partial Differential Equations, *J. Comput. Phys.*, vol. 82, pp. 454–486, 1989.
15. M. Lacroix, Numerical Solution of Phase Change Problems: An Eulerian-Lagrangian Approach, *Numer. Heat Transfer Part B*, vol. 19, pp. 57–78, 1992.
16. A. J. Wathen, Optimal Moving Grids for Time-Dependent Partial Differential Equations, *J. Comput. Phys.*, vol. 101, pp. 51–54, 1992.
17. V. I. Mazhukin, U. Semmler, P. V. Breslavskij, and L. Ju. Takojeva, Das Programmpaket LASTEC-1 zur Numerischen Simulation von Lasermaterialbearbeitungsprozessen, Internal Report 209/5, Technische Universität Chemnitz, 1991.
18. A. Lashin, I. Smurov, A. Uglov, P. Matteazzi, and V. Tagliaferri, Heat Process in Pulse Laser Treatment of Metallic Materials, *Int. J. Heat Technol.*, vol. 7, no. 2, pp. 60–73, 1989.
19. I. Smurov, A. Uglov, A. Lashin, P. Matteazzi, and V. Tagliaferri, Modelling of Pulse-Periodic Energy Flow Action on Metallic Materials, *Int. J. Heat Mass Transfer*, vol. 34, no. 4/5, pp. 961–971, 1991.
20. A. Uglov, I. Smurov, A. Lashin, and A. Guskov, *Modeling of Thermal Processes under Pulse Laser Action on Metals*, Nauka Publishers, Moscow, 1991.